Oncogene (2016) **35,** 4730–4740

www.nature.com/onc

ORIGINAL ARTICLE

Role of Runx2 in IGF-1Rβ/Akt- and AMPK/Erk-dependent growth, survival and sensitivity towards metformin in breast cancer bone metastasis

M Tandon, Z Chen, AH Othman and J Pratap

The mechanisms underlying reprogramming of growth factor signaling and metabolic pathways during bone metastasis of breast cancer are not clear. The Runt-related transcription factor (Runx2) regulates cell signaling during mammary epithelial morphogenesis and promotes invasion; therefore, we investigated its role in cell growth and metabolic signaling in bone-seeking breast cancer cells. We performed systemic inoculation of control or Runx2 knockdown invasive MDA-MB-231 cells in NOD/SCID mice, and compared parental and bone-derived variants for phenotypic and molecular alterations. The Runx2 knockdown showed early (0–2 weeks) inhibition of metastatic spread but late (4–6 weeks) outgrowth, suggesting Runx2-dependent bi-phasic response and reprogramming of metastatic cells. The late-stage tumor outgrowth of bone-derived Runx2 knockdown cells was associated with increased insulin-like growth factor- 1Rβ (IGF-1Rβ) levels. Interestingly, glucose uptake and glycolysis were reduced in the bone-derived Runx2 knockdown cells that could be further reduced by extracellular-regulated protein kinase (Erk1/2) inhibition. Furthermore, the Runx2 knockdown cells displayed activation of AMP-activated protein kinase (AMPKα), the sensor of cellular metabolism. Importantly, the Runx2 knockdown in bone-derived cells resulted in increased sensitivity to both Erk1/2 inhibition and AMPKα activation by PD184161 and metformin, respectively, despite increased IGF-1Rβ and AMPKα levels. Our results reveal that Runx2 promotes metastatic spread of mammary tumor cells. The growth of late-stage tumor cells can be targeted by Runx2 knockdown in combination with Mek-Erk1/2 inhibition and metformin treatment.

Oncogene (2016) **35,** 4730–4740; doi:10.1038/onc.2015.518; published online 25 January 2016

INTRODUCTION

Bone metastasis is associated with ~70% mortality in the advanced stages of breast cancer patients and reduction in quality of life.[1,2] During metastasis, the invasive breast cancer cells survive in the bone microenvironment due to pre-existing or acquired changes in cell signaling and metabolic pathways;[3–7] however, underlying regulatory mechanisms are still unknown.

The Runt-related transcription factor (Runx2), a critical factor for bone development,[8] is also aberrantly expressed in cancer cells compared with normal mammary epithelial cells,[9] where it regulates β-casein,[10] osteopontin,[11] sialoprotein,[12] calcitonin and RANKL.[13] Ectopic expression of Runx2 disrupts mammary acini formation in the three-dimensional (3D) culture model and Runx2 transgenic mice display alveolar hyperplasia, ductal carcinoma *in situ* and age-dependent preneoplastic changes.[14,15] In breast cancer patient specimens, Runx2 expression levels correlated to triple negative tumor status and poor clinical outcome.[15,16] Intriguingly, Runx2 suppresses proliferation of osteoblasts, and functions in both tumor suppressor-related and oncogene-related properties of breast and osteosarcoma cells.[17–19] These studies suggest context-dependent functions of Runx2 in cancer progression. However, the role of Runx2 in initial colonization and growth of tumor cells during bone metastasis is still unclear.

The bone microenvironment is conducive for tumor survival because it harbors several growth factors,[20] including insulin-like growth factors (IGFs). IGF-1, a potent mitogen, activates IGF-1Rβ receptor tyrosine kinase during bone metastasis.[21] The activation of IGF-1Rβ triggers downstream signaling including the PI3K/Akt pathway, a critical driver of tumor growth.[22] The IGF-1Rβ levels are increased in breast cancer metastasis and disruption of IGF-1/IGF-1R signaling inhibited tumorigenesis in preclinical models.[22–25] In addition to increased growth factor signaling, the tumor cells undergo metabolic reprogramming by altering glucose uptake or glycolysis.[26] Our previous studies and other reports demonstrated regulatory roles of Runx2 in growth factor signaling,[27] tumor cell migration[28,29] and survival during glucose deprivation.[9] However, Runx2-dependent crosstalk between growth factor and metabolic signaling pathway in bone metastasis is still unclear. Here we demonstrate Runx2-mediated IGF-1Rβ-pAkt and AMPK-Erk1/2 (extracellular-regulated protein kinase) signaling crosstalk in survival of bone-derived breast cancer cells. Importantly, Runx2 knockdown sensitizes these cells for Mek-Erk1/2 inhibition and metformin treatment.

RESULTS

Runx2 knockdown inhibits early metastatic spread but promotes late-stage tumor regrowth in bone

To determine the role of Runx2 in mammary tumor metastasis, we stably knockdown *Runx2* in high endogenous Runx2 expressing invasive MDA-MB-231 cells.[9] We observed up to 80% Runx2 suppression (Supplementary Figures S1A and B) and consistent

Department of Anatomy and Cell Biology, Rush University Medical Center, Chicago, IL, USA. Correspondence: Dr J Pratap, Department of Anatomy and Cell Biology, Rush University Medical Center, Armour Academic Center, 600 South Paulina Street, Suite 507, Chicago, IL 60612, USA.
E-mail: jitesh_pratap@rush.edu
Received 14 June 2015; revised 19 October 2015; accepted 11 December 2015; published online 25 January 2016

with the previous results,[7,28,30] the Runx2 knockdown resulted in delay in wound healing response indicating a positive role of Runx2 in cell migration (Supplementary Figure S1C). Next, we systemically inoculated luciferase-expressing control or Runx2 knockdown cells in NOD/SCID mice via intra-cardiac route and quantified the metastatic outgrowth by bioluminescence imaging (Figure 1a). The Runx2 knockdown cells showed an early decline (week 1, 45%, $P < 0.05$ and week 2, 36%, $P < 0.1$) in overall metastatic outgrowth compared with the control cells (Figure 1b). However, at later time (weeks 4–6), the Runx2 knockdown cells showed significantly upregulated (week 4, 75%, $P < 0.05$; week 5, 60%, $P < 0.05$ and week 6, 36%, $P < 0.1$) overall metastatic outgrowth (Figure 1b). No significant differences were noted at week 3, suggesting a shift in growth rate of Runx2 knockdown cells. These results could not be accounted due to differences in the luciferase expression among these cells (Supplementary Figure S1D). Although tumor growth was observed in multiple sites including brain, liver and kidney, we stratified the overall bioluminescence signal to lungs and bones, the most common sites of breast cancer metastasis (Supplementary Figure S1E). The bone metastasis incidences were nearly doubled and tumor growth in bone was observed in the Runx2 knockdown group at later time point (Supplementary Figures S1F and G). For lung metastasis, Runx2 knockdown showed 40% reduced incidences with a modest twofold increase in tumor growth. To determine the tumor growth associated bone loss, we performed X-ray and microcomputed tomography (μCT) analysis on long bones (femur and tibia). These analyses revealed that late-stage regrowth of Runx2 knockdown cells are associated with osteolytic lesions in proximal tibia and cortical bone loss (Figure 1c and Supplementary Figure S1H). To quantify the bone loss, we performed 3D rendering of the trabeculae distal to the growth plate in proximal tibia by μCT. This analysis indicated that trabecular bone volume fraction and connectivity was significantly reduced in the Runx2 knockdown group compared with controls (Figure 1d and Supplementary Figure S1I). Taken together, these results suggest a bi-phasic role of Runx2 during tumor metastasis, wherein Runx2 loss delays tumor cell migration, metastasis at early (1–2 weeks) stages, while it enhances tumor growth in bone and osteolysis at later stages (4–6 weeks).

Bone-derived Runx2 knockdown cells show increased IGF-1Rβ expression levels

To understand the role of Runx2 in late-stage metastatic outgrowth in bones, we investigated the growth factor receptor signaling. To achieve this, we isolated these tumor cells from mice 6 weeks post-injection, and compared tumor-derived and parental cells to determine alterations in growth factor receptor signaling. The IGF-1Rβ expression levels were significantly upregulated in bone-derived Runx2 knockdown cells compared with matched bone-derived control cells (Figure 2a, right). In contrast, the epidermal growth factor receptor levels were reduced (20–50%) in lung or bone-derived cells (Supplementary Figure S2A). Furthermore, IGF-1Rβ levels were similar in parental population or lung-derived Runx2 knockdown cells, suggesting that increased IGF-1Rβ levels could specifically facilitate late-stage tumor growth in bone due to loss of Runx2. To determine the activity of IGF-1Rβ

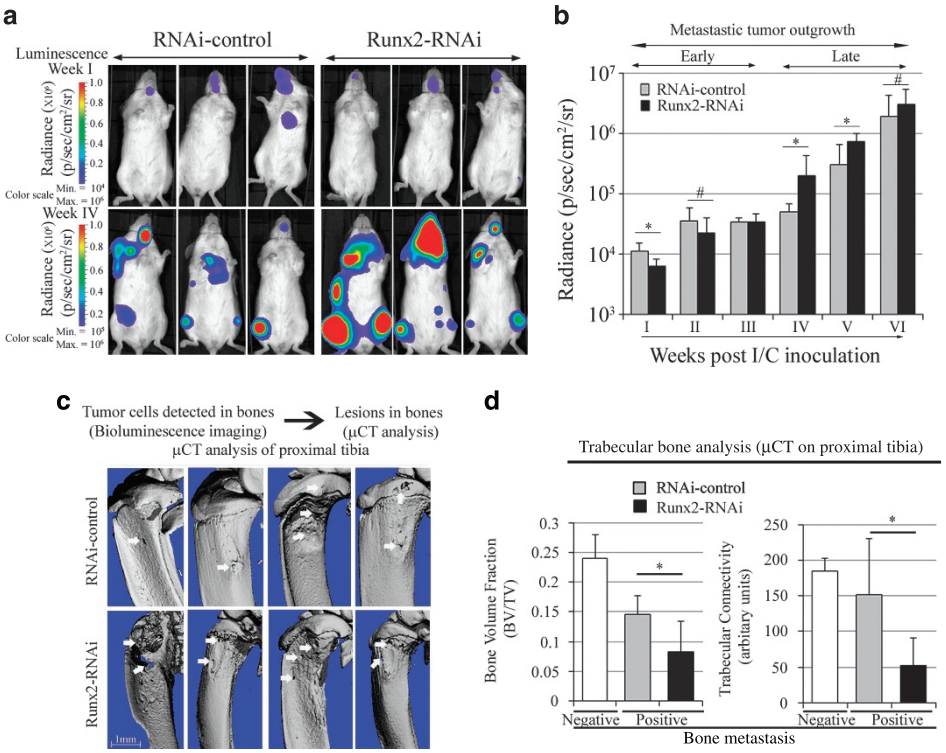

Figure 1. A Runx2-dependent metastatic outgrowth of MDA-MB-231 cells in NOD/SCID mice. (**a**) The control or Runx2 knockdown MDA-MB-231 cells were inoculated i/c into NOD/SCID mice ($n = 10$ per group) and overall metastatic outgrowth was monitored by bioluminescence imaging. The blue–red pseudocolor for radiance indicates the presence of luciferase-expressing cells in three representative mice at early (week 1) and late (week 4) time points. (**b**) The overall tumor outgrowth in mice was quantified by drawing regions of interest as indicated in the Materials and methods section. The experiments were repeated twice and the average of three independent experiments ($n = 14$–24) is shown. (**c**) The designated mice, inoculated with control or Runx2 knockdown MDA-MB-231 cells, showing bioluminescent signal in long bones were killed and the preserved bones were examined for osteolytic lesions by μCT. The arrow indicates the presence of osteolytic lesions; scale bar is 1mm. (**d**) The osteolysis was quantified by generating 3D trabecular architecture distal to the growth plate (Supplementary Figure S1I). The bone volume fractions and trabecular connectivity were estimated in mice bearing control or Runx2 knockdown cells in the proximal tibia and shown relative to the normal bone (bioluminescent signal negative). $^{*}P \leq 0.05$, $^{\#}P \leq 0.1$ in unpaired Student's *t*-test.

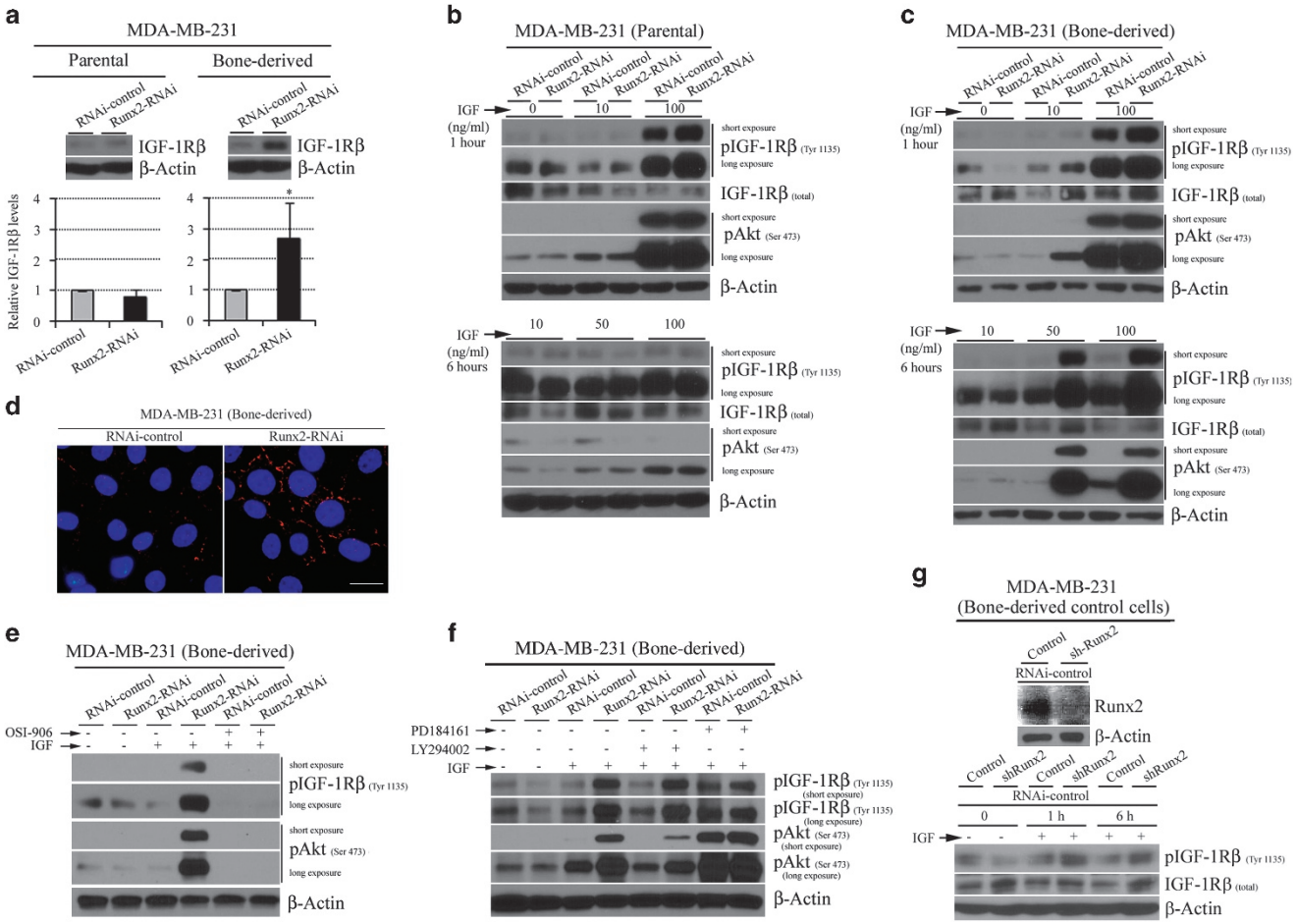

Figure 2. Runx2 knockdown increases IGF-1Rβ expression and PI3K/Akt signaling in bone-derived MDA-MB-231 cells. (**a**) The mice harboring control or Runx2 knockdown MDA-MB-231 tumors in bone were killed and cells were collected, cultured and enriched as indicated in Materials and methods section. The whole-cell lysates from parental (preinoculated) and bone-derived control or Runx2 knockdown cells were examined for IGF-1Rβ expression by western blotting. The β-actin expression was utilized as an internal control to normalize expression levels. The quantification of the IGF-1Rβ expression level from at least three independent experiments is shown in the lower panel. * indicates *P*-value ≤ 0.05 in unpaired Studen'st *t*-test. (**b**, **c**) The parental (**b**) or bone-derived (**c**) control or Runx2 knockdown cells were deprived of serum for 16 h and then stimulated with IGF-1 as indicated. The expression levels of total, pIGF-1Rβ and pAkt were examined with β-actin as an internal control. (**d**) The pIGF-1Rβ localization in bone-derived control or Runx2 knockdown MDA-MB-231 cells was determined by immunofluorescence. The red signal (Alexa Fluor 594) indicates pIGF-1Rβ, and the while blue signal from 4′, 6-diamidino-2-phenylindole (DAPI) shows nucleus; scale bar is 20 μm. (**e**, **f**) The bone-derived control or Runx2 knockdown cells were serum-deprived and stimulated with IGF-1 in the presence or absence of selective IGF-1Rβ inhibitor OSI-906, PI3K inhibitor LY294002 and Mek inhibitor PD184161 for 1 h. The pIGF-1Rβ and pAkt expression levels were determined by western blotting, while β-actin expression was utilized as a loading control. (**g**) The bone-derived control cells were reinfected with Runx2 shRNA lentivirus vectors and Runx2 knockdown was confirmed (upper panel). The IGF-1-treated cells were examined for pIGF-1Rβ and total IGF-1Rβ expression levels, while β-actin was utilized as an internal control.

signaling pathway, the serum-deprived cells were stimulated with IGF-1. The basal levels of IGF-1Rβ phosphorylation (pIGF-1Rβ) in serum-deprived conditions were either undetectable or present in low levels and were reduced in bone-derived Runx2 knockdown cells. As expected, the IGF-1 stimulation for 1 h showed potent and dose-dependent induction of pIGF-1Rβ and downstream pAkt in both parental and bone-derived Runx2 knockdown or control cells (Figures 2b and c, upper panels). Importantly, the bone-derived Runx2 knockdown cells showed prolonged ($\geqslant$6 h) pIGF-1Rβ and pAkt levels upon IGF-1 stimulation compared with control or parental cells (Figures 2b and c, lower panels). We observed variation in total IGF-1Rβ levels upon IGF-1 treatment at various time points examined that could be related to receptor internalization and turnover.[31] However, the bone-derived Runx2 knockdown cells displayed higher total IGF-1Rβ levels compared with control cells at every time point examined. Consistent with membrane localization,[22] we also observed that pIGF-1Rβ was predominantly localized at cell boundaries (Figure 2d). Next, to determine if the increase in pAkt levels are dependent upon IGF-1-mediated pIGF-1Rβ expression levels or crosstalk with the Mek-Erk1/2 pathway,[27] we utilized OSI-906 (Linsitinib), LY294002 and PD184161, selective inhibitors of pIGF-1Rβ, PI3K/Akt and Mek-Erk1/2 signaling, respectively. Indeed, the IGF-1-mediated induction of pIGF-1Rβ and pAkt levels in bone-derived Runx2 knockdown cells was completely abrogated by OSI-906 treatment confirming that pAkt induction is dependent upon IGF-1-mediated pIGF-1Rβ (Figure 2e). Additionally, LY294002 treatment reduced pAkt levels suggesting that PI3K activity is required for IGF-1Rβ-induced pAkt, while PD184161 treatment increased pAkt levels (Figure 2f). Finally, to validate that bone microenvironment enhanced IGF-1Rβ levels and downstream signaling upon Runx2 depletion, we examined IGF-1Rβ levels in non-bone-derived and bone-derived cancer cell lines. The Runx2 knockdown in bone-derived control MDA-MB-231 cells (Figure 2g) and prostate cancer PC3 cell line, but not in breast carcinoma-derived Hs578t cells (Supplementary Figure S2B) showed increased pIGF-1Rβ levels

upon IGF-1 treatment at various time points. The reinoculation of Runx2 knockdown cells in *ex vivo* bone co-cultures (Supplementary Figure S3A) showed further increased pIGF-1Rβ levels compared with bone-derived cells (Figure 3a). Interestingly, the IGF-1Rβ mRNA levels were not altered significantly with Runx2 knockdown (Supplementary Figure S3B). Furthermore, the Runx2 knockdown in bone-derived MDA-MB-231 cells was not affected by IGF-1 or inhibitor treatments (Supplementary Figure S3C). Altogether, these results show that the late-stage metastatic outgrowth of Runx2 knockdown cells in bone is associated with increased IGF-1Rβ signaling.

Bone-derived Runx2 knockdown cells show reduced Erk1/2 levels and altered expression of IGF-1Rβ pathway genes

Previously, we and others have demonstrated that crosstalk between Mek-Erk1/2 and PI3K-Akt pathways upregulates growth factor receptor levels in mammary epithelial cells.[27,32] Furthermore, consistent with our previous findings,[9] our results show increased pAkt levels upon Mek inhibitor PD184161 treatment (Figure 2f). Therefore, we determined endogenous Erk1/2 levels and downstream target genes of IGF-1Rβ/Akt signaling. The total and pErk1/2 levels were reduced in bone-derived Runx2 knockdown cells (Figures 3a and b). Next, to determine whether altered pErk1/2 and IGF-1Rβ levels are due to clonal selection, we examined single-cell-derived colonies isolated from both parental and bone-derived MDA-MB-231 populations. These colonies showed varying expression levels of pErk1/2, pIGF-1Rβ and total IGF-1Rβ (Figure 3c). The quantification of the expression level of these proteins in six clones revealed reduced pIGF-1Rβ and total IGF-1Rβ levels in Runx2 knockdown parental cells compared with control (Figure 3d). Importantly, colonies from Runx2 knockdown bone-derived cells displayed variable and reduced pErk1/2 but increased pIGF-1Rβ levels compared with control cells (Figures 3c, lower panel and d). These results suggest that the increase in pIGF-1Rβ/pAkt signaling in bone-derived cells is not due to selection of a clonal population in bone.

To determine the expression levels of downstream target genes of the IGF-1Rβ pathway, we analyzed pathway-related genes in a PCR array and compared bone-derived Runx2 knockdown cells with control and parental cells. We identified eight genes showing $\geqslant$ 2-fold upregulation including *c-Fos* that showed a sevenfold increase (Figure 3e). We validated the array data by utilizing alternate primer sets in reverse transcriptase–PCR and western blot analysis (Figures 3f and g). The induction of *c-Fos* is consistent with the IGF-1/IGF-1Rβ-responsive differential gene expression changes that facilitate cancer progression.[33] Additionally, expression of other PI3K/Akt signaling target genes such as apoptosis

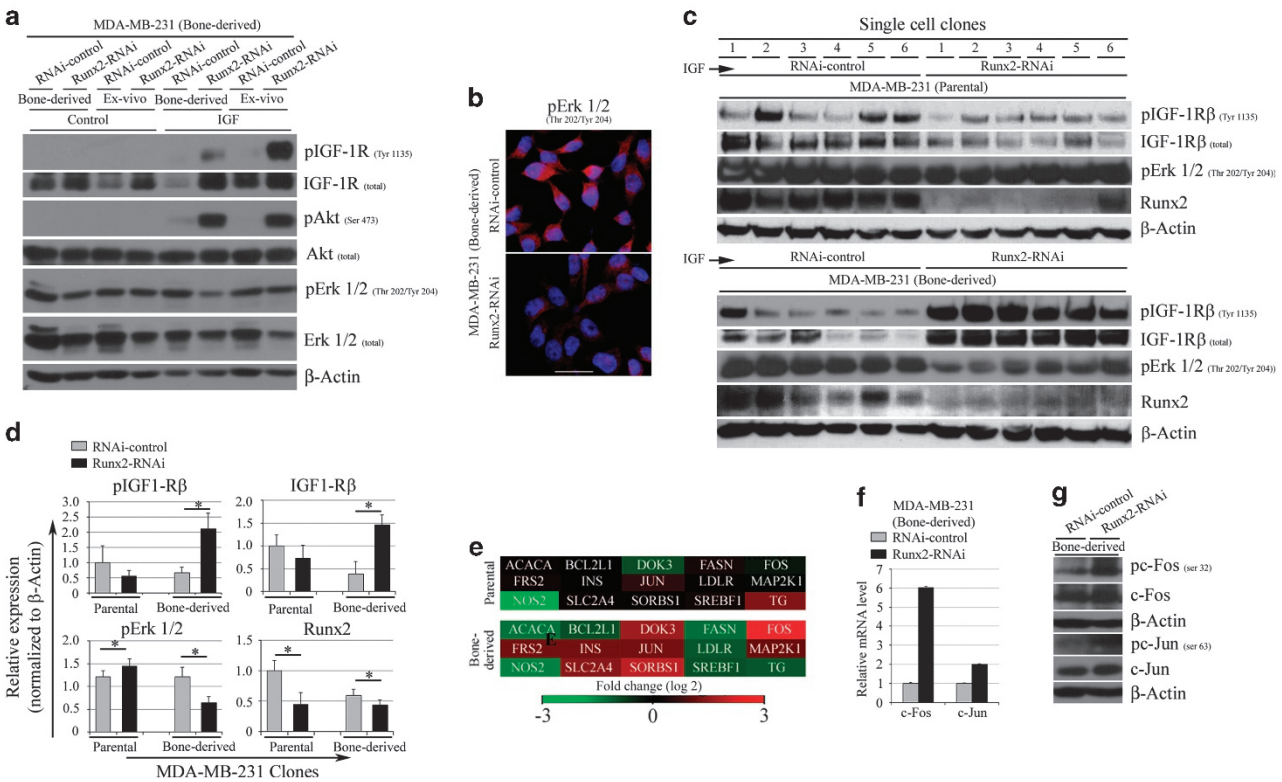

Figure 3. Runx2 knockdown-mediated increase in IGF-1Rβ expression in bone-derived MDA-MB-231 cells is not due to clonal selection. (**a**) The bone-derived control or Runx2 knockdown MDA-MB-231 cells were co-cultured *ex vivo* in bone (Supplementary Figure S3) as indicated in Materials and methods section. The whole-cell lysates from serum-deprived and IGF-1-treated cells were prepared and examined for pIGF-1Rβ, total IGF-1Rβ, pAkt, pErk1/2 and total Erk1/2 protein expression levels by western blotting. (**b**) The pErk1/2 localization in bone-derived control and Runx2 knockdown cells was analyzed by immunofluorescence staining of fixed cells. The red color (AF-594) indicates predominant cytoplasmic localization of pErk1/2, and the while blue (DAPI) indicates nucleus, scale bar is 20 μm. (**c**) The single-cell clonal populations were isolated from parental and bone-derived control or Runx2 knockdown cells. The whole-cell lysates from serum-deprived and IGF-1-stimulated control or Runx2 knockdown clonal populations (numbered on top) were prepared. The IGF-1Rβ, pErk1/2 and Runx2 expression levels were determined by western blotting, while β-actin expression was utilized as a loading control. (**d**) The quantifications of pIGF-1Rβ, total IGF-1Rβ, pErk1/2 and Runx2 levels from six clonal populations relative to β-actin levels is shown. (**e**) The expression levels of a panel of IGF-1 signaling target genes in the PCR array were analyzed in parental or bone-derived control and Runx2 knockdown cells by real-time PCR. The normalized mRNA expression levels of selected genes with over twofold change are indicated with pseudocolor in heat map. (**f**, **g**) The gene expression levels of c-Fos and c-Jun were validated by reverse transcriptase–PCR utilizing alternate primers, while protein expression was determined by western blotting.

inhibitor *Bcl2l1* and genes linked to fatty acid and cholesterol metabolism (*ACACA, FASN, LDLR, SREBF1*) was reduced in bone-derived Runx2 knockdown. Taken together, our results show that increased pIGF-1Rβ/pAkt signaling and altered expression of IGF-1Rβ responsive genes in Runx2 knockdown cells are associated with Erk1/2 downregulation.

Increased IGF-1Rβ and reduced Erk1/2 expression levels in bone-derived Runx2 knockdown cells are due to loss of β-Arrestin-1/2 expression

To understand how IGF-1Rβ and Erk1/2 expression levels are coupled to loss of Runx2 in bone-derived cells, we examined the levels of β-Arrestins, downstream adapter proteins that promote IGF-1Rβ internalization and ubiquitination.[34] The *β-Arrestin-1/2* gene expression was reduced by fivefold and nearly 50–75% reduction in protein expression was observed in bone-derived Runx2 knockdown cells compared with control and parental cells (Figures 4a–c). The decline in β-Arrestin-1/2 was not affected by stimulating or inhibiting IGF-1Rβ or Erk1/2 signaling (Figure 4d). Therefore, to determine whether Runx2 regulates *β-Arrestin-1/2* expression, a *β-Arrestin-1* promoter fragment (+250 bp) containing putative Runx-binding sequences was cloned upstream of luciferase reporter (Supplementary Figure S4). The overexpression of WT-Runx2 in MDA-MB-231 or HeLa cells showed nearly twofold increase in luciferase reporter activity (Figures 4e and f). The HeLa cells were included in this analysis because these cells lack endogenous Runx2.[35] Since *β-Arrestin-1/2* expression was substantially reduced only in bone-derived Runx2 knockdown cells but not in parental cells, we tested a possibility of epigenetic regulation of β-Arrestin-1/2 in bone-derived cells. First, we examined the global histone acetylation levels and found that acetylation of Histone H3 (lysine 9) was reduced by 30% in

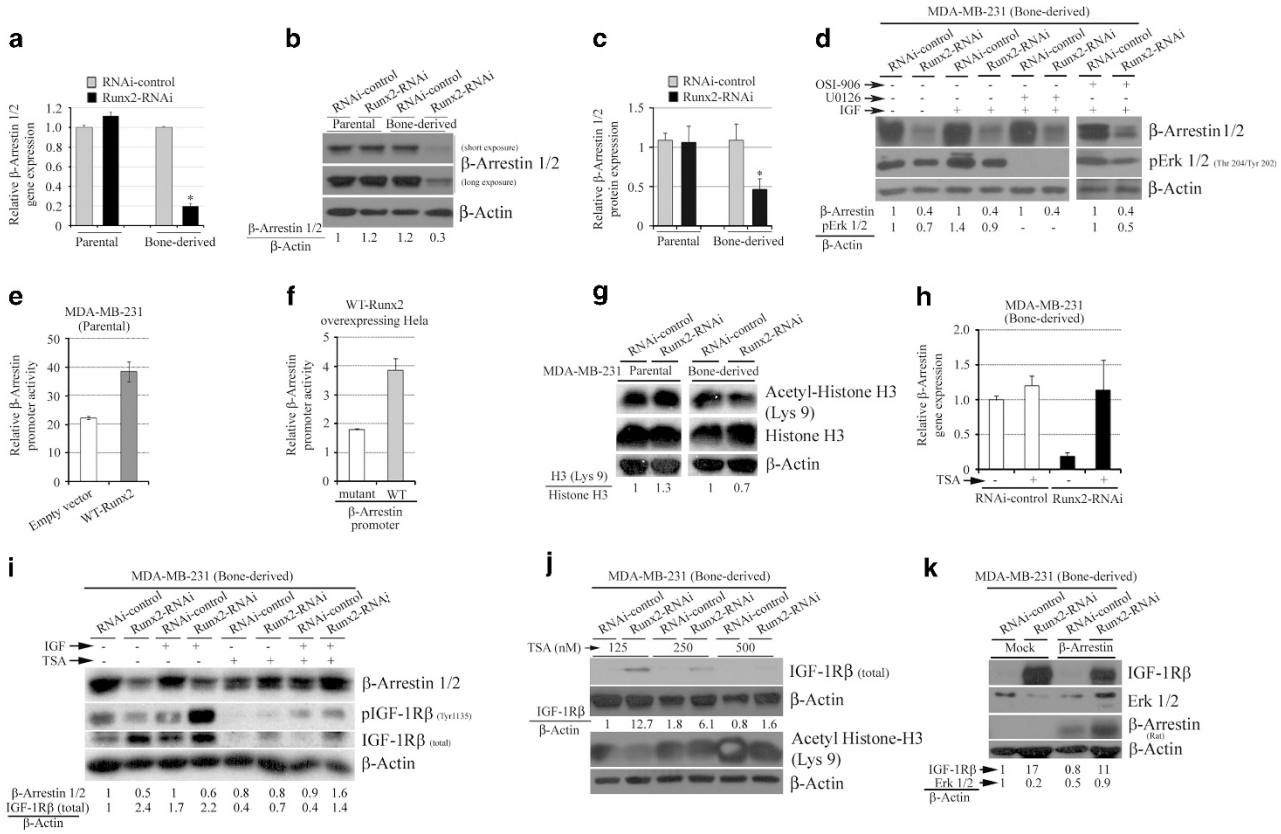

Figure 4. Runx2 knockdown increases IGF-1Rβ expression by downregulating β-Arrestin expression in bone-derived MDA-MB-231 cells. (**a**) The β-Arrestin-1/2 gene expression in indicated parental or bone-derived MDA-MB-231 cells was determined by reverse transcriptase–PCR. The data were normalized by 28S as an internal control and relative ΔΔCt quantifications are shown. (**b**, **c**) The whole-cell lysates from parental or bone-derived, control and Runx2 knockdown MDA-MB-231 cells were prepared. The β-Arrestin-1/2 expression was determined by western blotting, while β-actin expression was utilized as an internal loading control. The average expression levels ($n = 4$) are shown, * indicates $P \leq 0.05$. (**d**) The bone-derived control or Runx2 knockdown cells were serum deprived for 16 h and then stimulated with IGF-1 in the presence or absence of OSI-906 and U-0126. The expression levels of β-Arrestin-1/2 and Erk1/2 were determined by western blotting. The quantifications relative to the β-actin expression level are shown below respective lanes. (**e**, **f**) The β-Arrestin promoter sequence bearing putative Runx-binding sites was cloned upstream of Firefly luciferase gene (Supplementary Figure S4) and transfected in MDA-MB-231 cells (**e**) or HeLa cells (**f**) expressing WT-Runx2 along with *Renilla luciferase*-expressing vector as an internal transfection control. An empty vector was utilized as control for WT-Runx2 expression, while Runx-binding sites were mutated to detect nonspecific promoter activity. The β-Arrestin promoter activity due to WT-Runx2 expression was determined in dual luciferase assays. (**g**) The whole-cell lysates from parental or bone-derived control and Runx2 knockdown cells were analyzed for total or acetylated histone H3 levels by western blotting. The β-actin expression level was utilized as an internal control and normalized quantifications are shown below respective lanes. (**h**) The bone-derived control or Runx2 knockdown cells were treated with TSA (62.5 nM) for 48 h and mRNA was isolated. The β-Arrestin-1/2 gene expression normalized to glyceraldehyde-3-phosphate dehydrogenase (GAPDH) was determined by real-time PCR analysis. (**i**, **j**) The bone-derived control or Runx2 knockdown cells were treated with various doses of TSA from 62.5 nM (I) or 125–500 nM (J) for 48 h. The whole-cell lysates were analyzed for IGF-1Rβ and H3 histone acetylation, while β-actin served as an internal control. (**k**) The bone-derived control or Runx2 knockdown MDA-MB-231 cells were transfected with pcDNA3.1 β-Arrestin-1 plasmid, while empty pcDNA3.1 plasmid was used as mock transfection. The IGF-1Rβ and Erk1/2 levels were determined by western blotting. The β-actin normalized quantification is shown below respective lanes. Abbreviation: TSA, Trichostatin A.

bone-derived Runx2 knockdown cells (Figure 4g). Second, we tested whether treatment of bone-derived cells with Trichostatin A, a selective inhibitor of histone deacetylases and activator of histone H3 acetylation, rescues the β-Arrestin-1/2 gene expression. Indeed, the Trichostatin A treatment in bone-derived Runx2 knockdown cells elevated the *β-Arrestin-1/2* gene expression level comparable to control cells (Figure 4h). Furthermore, the Trichostatin A treatment reduced total IGF-1Rβ levels in bone-derived Runx2 knockdown cells to the level of control cells (Figures 4i and j). Altogether, these results suggest that combination of decreased acetylation and loss of Runx2 reduces β-Arrestin-1/2 expression and increases IGF-1Rβ protein levels. Finally, to genetically validate these results, we overexpressed rat *β-Arrestin-1* in bone-derived MDA-MB-231 cells. The *β-Arrestin-1* overexpression reduced IGF-1Rβ and increased Erk1/2 levels (Figure 4k). These results confirm that Runx2 inhibits IGF-1Rβ levels and increases Erk1/2 expression by regulating β-Arrestin-1/2.

Runx2 knockdown increases sensitivity towards pharmacologic Erk1/2 inhibition

The altered levels of pIGF-1Rβ and pErk1/2 proteins in bone-derived Runx2 knockdown cells led to the hypothesis that these cells may be susceptible to targeting kinase activity. Therefore, we treated these cells with pharmacologic inhibitors and examined cell viability. The PD184161 treatment, but not OSI-906 or LY294002, showed loss of cell viability in MTT assays in both parental and bone-derived cells and was independent of Runx2 levels (Figure 5a, left and center panel). Since Runx2 knockdown reduced pErk1/2 levels (Figures 3a–d), we next tested sensitivity of these cells to lower doses of PD184161. The PD184161 treatment in bone-derived Runx2 knockdown cells showed more than twofold reduction in MTT absorbance after 48 h, while the hemocytometer cell counts were minimally reduced or unchanged compared with control cells (Figure 5a, right panel and Supplementary Figure S5A). These results suggested that metabolism could be altered in Runx2 knockdown cells since MTT is based on bio-reduction of tetrazolium compound and reflects the rate of glycolytic NADH production in metabolically active cells.[36]

Since MDA-MB-231 cells are predominantly glycolytic,[37,38] we next tested Runx2-dependent changes in metabolism by measuring glucose uptake and glycolytic capacity. The Runx2 knockdown cells revealed lower glucose uptake in both parental and bone-derived cells compared with controls (Figure 5b). Although, glycolysis, as indicated by the extracellular acidification rate, was reduced in bone-derived cells, no Runx2-dependent changes were observed (Figure 5c, left). However, treating bone-derived Runx2 knockdown cells with PD184161 resulted in significant reduction of extracellular acidification rate (Figure 5c, right). Next, we determined phenotypic changes after long-term pharmacologic IGF-1Rβ and Erk1/2 inhibition. The bone-derived Runx2 knockdown cells treated with OSI-906 showed reduced colony size compared with vehicle-treated controls (Figure 5d), while treatment with PD184161 resulted in no colony formation or anchorage-independent cell growth (Figure 5e). Taken together, these results suggest that long-term pharmacologic IGF-1Rβ inhibition can reduce cell growth but not survival and that can be effectively targeted by inhibition of the Mek-Erk1/2 pathway.

Runx2 knockdown potentiates metformin-induced energy metabolism and inhibition of cell viability

To understand how Runx2 knockdown cells survive in bone microenvironment despite reduced glucose uptake and glycolysis, we examined adaptive modifications in regulation of energy metabolism. The AMP-activated protein kinase (AMPKα) is a ubiquitous regulator of energy homeostasis and its phosphorylation is triggered by glucose stress or hypoxia in tumor microenvironment.[39] The basal levels of pAMPKα were higher (2.8-fold) in bone-derived Runx2 knockdown cells compared with control (Figures 6a and b), suggesting that these cells are responding to metabolic stress. The increase in pAMPKα levels persisted in the presence of IGF-1 or insulin treatment (Figure 6c), while the total AMPKα protein levels were not significantly altered with Runx2 knockdown (Supplementary Figure S5B). It has been suggested that the extent and duration of AMPKα activation could induce growth arrest or cell death.[40] Therefore, to examine whether further increase in pAMPKα levels promote cell death, we treated these cells with metformin. Previous studies have shown potent antiproliferative effects of metformin via AMPKα activation and Erk1/2 inhibition in triple negative cell lines.[41–43] We reasoned that Runx2 knockdown in bone-derived cells showing high pAMPKα and low Erk1/2 should potentiate the metabolic and growth inhibitory effects of metformin. The metformin treatment in bone-derived MDA-MB-231 cells resulted in further increase in pAMPKα levels and decrease in Erk1/2 levels in Runx2 knockdown cells (Figures 6d–f and Supplementary Figures S5C and D). Notably, Runx2 knockdown in bone-derived cells showed reduced p-p70S6K in basal and metformin-treated conditions compared with control cells. The selective AMPK inhibitor Compound C[44] mitigated pAMPKα activation and p-p70S6K reduction. Furthermore, metformin treatment reduced the IGF-1Rβ levels in bone-derived Runx2 knockdown cells in dose- and time-dependent manner (Figure 6g) coupled with significant cellular rounding, cytoskeletal condensation and reduced cell growth (Figure 6h). Consistently, the increase in p-p70S6K has been shown to decrease cell circularity and promote adhesion.[45] At various doses (0.2–5 mM), metformin treatment did not show Runx2-dependent effect on cell proliferation (Supplementary Figure S5A); however, significantly reduced metabolism was observed in bone-derived Runx2 knockdown cells (Figure 6i) as determined by MTT assays. The reduction in β-Arrestin-1/2 levels was not affected by metformin treatment in these cells (Figures 6e and f). Therefore, the decline p-p70S6K and increase in pAMPKα suggest that Runx2 knockdown induces stress response in metastatic cells. Altogether, our results in bone-derived MDA-MB-231 cells indicate that loss of Runx2 potentiates the effect of AMPKα activation or Mek-Erk1/2 inhibition in regulating tumor cell metabolism and growth.

DISCUSSION

We identified a novel regulatory function of Runx2 that integrate IGF-1Rβ/Akt and AMPKα/Erk signaling crosstalk in growth of bone-derived metastatic breast cancer cells (Figure 7). The bone microenvironment provides enriched growth factor environment;[4,46,47] however, the signaling response of metastatic cancer cells to these conditions in bone is still unclear. Here, we characterized bone-derived MDA-MB-231 cells after systemic inoculation of parental population. We found that Runx2 loss delays early metastatic spread of these cells. The late-stage growth of Runx2 knockdown cells is associated with activation of IGF-1Rβ and AMPKα signaling. Importantly, Runx2 loss sensitizes bone-derived MDA-MB-231 cells to Mek-Erk1/2 inhibition and metformin treatment. Our results highlight Runx2 as a potential therapeutic target in combination with metformin or Mek-Erk1/2 inhibitors for bone metastasis.

The ligand IGF-1 from bone matrix binds and activates IGF-1Rβ to promote tumor cell survival and growth.[48,49] Our results show that the total IGF-1Rβ level increases due to reduced β-Arrestin-1/2 in Runx2 knockdown bone-derived MDA-MB-231 cells, and prolongs IGF-1Rβ/Akt signaling upon IGF-1 stimulation compared with parental cells (Figure 2). Previously, we showed that Runx2 loss in parental MDA-MB-231 cells reduces mTORC2 and diminishes epidermal growth factor-dependent Akt activation.[9] Since Akt

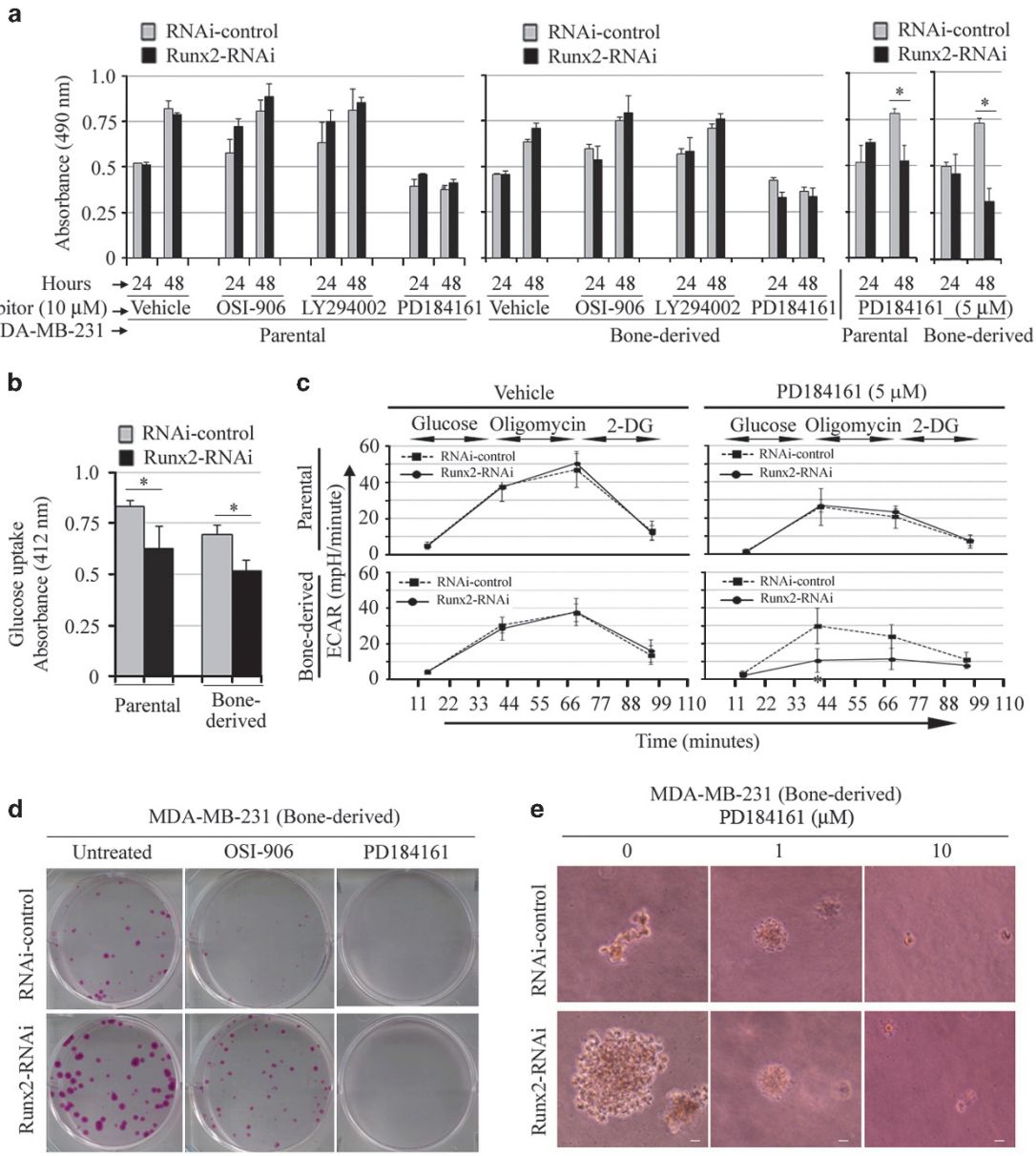

Figure 5. Runx2 knockdown enhances sensitivity towards pharmacologic Mek-Erk1/2 inhibition in bone-derived MDA-MB-231 cells. (**a**) The parental or bone-derived control and Runx2 knockdown MDA-MB-231 cells were seeded in a 96-well dish (10 000 cells per well) containing normal growth media with 10% fetal bovine serum (FBS) in the absence (vehicle, dimethyl sulfoxide) or presence of OSI-906, LY294002 and PD184161 as indicated. The MTT assay was performed after 24 or 48 h and the absorbance was recorded. * indicates $P \leq 0.05$ in unpaired Student's *t*-test. (**b**) The glucose uptake in parental or bone-derived Runx2 knockdown or control MDA-MB-231 cells was determined using glucose analog 2-deoxyglucose (2-DG) in a colorimetric assay. (**c**) The glycolysis in parental or bone-derived Runx2 knockdown or control MDA-MB-231 cells was determined in real time by inducing acute metabolic stress. The extracellular acidification rate was determined after sequential administration of glucose, oligomycin and 2-DG in a *Seahorse* extracellular flux analyzer. (**d**, **e**) The bone-derived control or Runx2 knockdown cell were seeded for *in vitro* anchorage-dependent (100 cell/well in a six-well culture plate in triplicates) (**d**) or anchorage-independent soft agar colony formation assays (100 cells/well in a six-well culture plate) (**e**). After 14 days, the colonies were stained with crystal violet and photographed (**d**) or unstained colonies were imaged in a brightfield microscope at ×40 magnification (**e**). The experiments were repeated twice; scale bar is 20 μm.

is one of the central node of multiple growth factor signaling and glucose metabolism,[50] our results suggest that Runx2 levels are important to balance growth factor signaling depending upon microenvironment and metabolic status of cancer cells.

The clinical trials targeting IGF-1R have not achieved desired outcome,[51] presumably due to lack of patient stratification or resistance to small molecules. We show that blocking the activity of Mek-Erk1/2, but not IGF-1Rβ, inhibits survival of high IGF-1Rβ-expressing Runx2 knockdown bone-derived MDA-MB-231 cells (Figures 5d and e). Our results demonstrate that despite increased IGF-1Rβ signaling, the bone-derived Runx2 knockdown cells were sensitive for pharmacologic Mek inhibition, and thus indicating their dependency on Mek-Erk1/2 pathway for survival. Taken together, our results suggest that tumors with high IGF-1R signaling may be effectively targeted by the Mek-Erk1/2 pathway inhibitors.

The Runx2-mediated regulation of target genes depends on its co-regulatory complex.[52] We show that the Runx2-β-Arrestin-1/2 axis operates in bone derived but not in parental MDA-MB-231 cells. The differential regulation of β-Arrestin-1/2 could be due

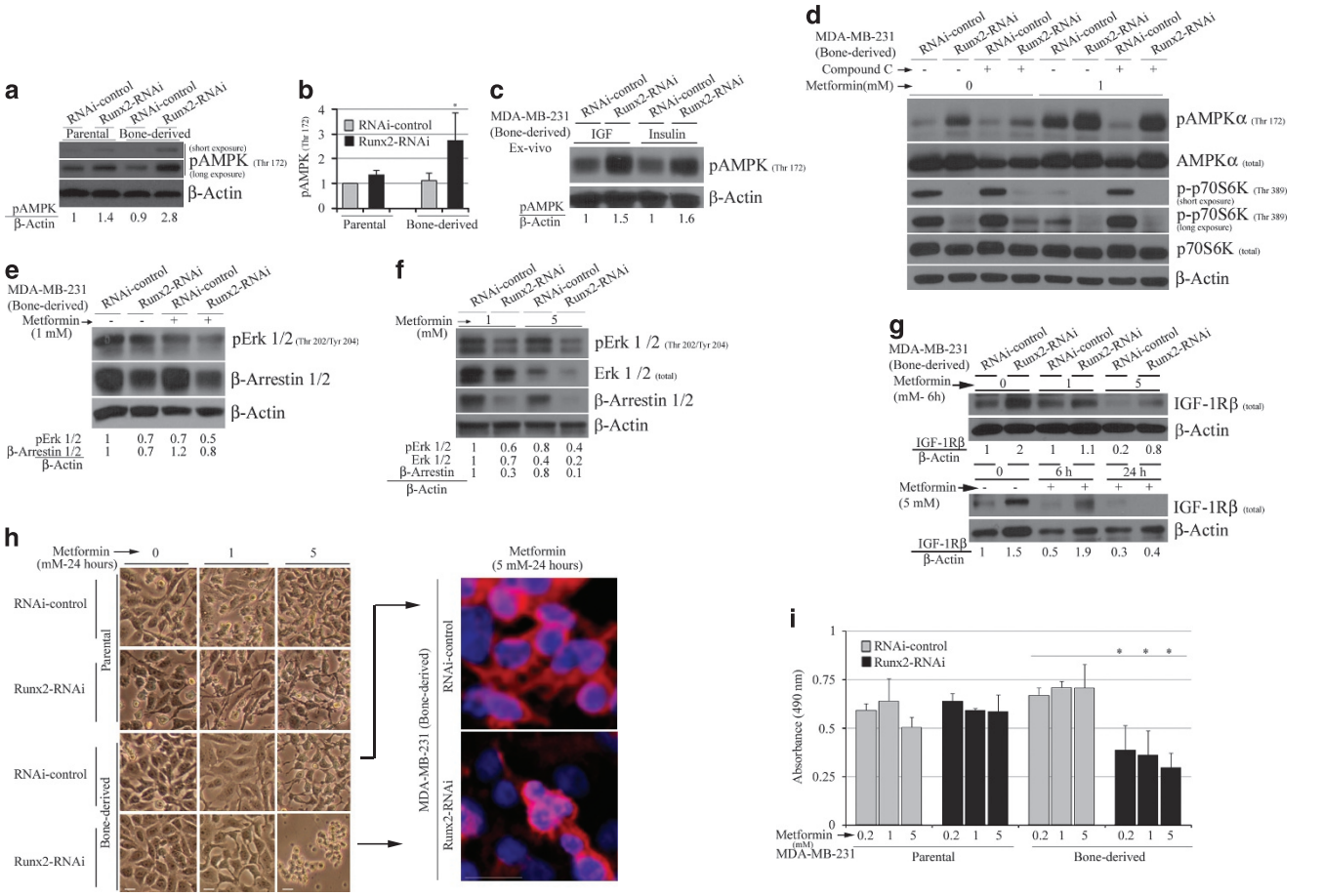

Figure 6. Runx2 knockdown increases sensitivity towards metformin treatment and inhibition of cell viability. (**a**, **b**) The parental and bone-derived Runx2 knockdown MDA-MB-231 cells were serum deprived and pAMPK expression levels were determined by western blotting (**a**). The β-actin expression levels were utilized as an internal control. The normalized expression levels are indicated below each lane and average quantification is shown ($n = 4$) (b). (**c**) The *ex vivo* bone-derived cells were treated with IGF-1 or insulin and pAMPK expression levels were determined by western blotting. (**d**) The bone-derived control or Runx2 knockdown cells were treated with metformin in the presence or absence of Compound C as indicated. The expression levels of pAMPK, total AMPK, p-p70S6k and total p70S6K were determined by western blotting on whole-cell lysates. (**e**–**g**) The bone-derived control or Runx2 knockdown cells were treated with metformin as indicated. The expression levels of pErk1/2, total Erk1/2, β-Arrestin-1/2 and total IGF-1Rβ were determined by western blotting. The β-actin normalized expression levels are shown below each lane. (**h**) The parental or bone-derived control or Runx2 knockdown MDA-MB-231 cells were cultured in the presence or absence of metformin for 24 h. The increase in cell rounding in bone-derived Runx2 knockdown cells was captured by brighfield microscopy. The cells were fixed and stained with phalloidin (red: actin cytoskeleton) and DAPI (blue: nucleus); scale bar is 20 μm. (**i**) The parental or bone-derived control and Runx2 knockdown MDA-MB-231 cells were seeded in a 96-well dish (10 000 cells per well) containing normal growth media with 10% FBS in the absence or presence of metformin as indicated. The MTT assay was performed after 24 h and the absorbance was recorded. * indicated $P \leq 0.05$ in unpaired Student's *t*-test.

to altered Runx2 co-regulatory complex[53] via post-translational modifications of Runx2[54,55] or epigenetic regulation of β-Arrestin promoter. In addition to Runx2, glucocorticoids have been shown to differentially regulate β-Arrestin-1/2 gene expression.[56] The decline in acetylated histone H3 in bone-derived Runx2 knockdown cells indicated epigenetic change that could alter β-Arrestin regulation. These epigenetic changes could be due to context-dependent activity of histone deacetylases and Runx2. Previous reports indicate that Runx2 not only physically interacts with epigenetic regulators such as (HDAC-1, HDAC-6, p300)[57–61] but can also regulate transcription of methyl transferases (e.g., *Ezh2*),[62] thereby altering histone modification. The treatment with Trichostatin A, an inhibitor of histone deacetylase activity, in bone-derived Runx2 knockdown cells restored the loss of *β-Arrestin-1/2* expression (Figure 4h). Furthermore, Runx2 activity is affected by post-translational modifications such as phosphorylation on serine and threonine residues, acetylation and sumoylation as shown in osteoblastic lineage cells,[55,63,64] prostate cancer cell lines and patient samples.[65] Taken together, these reports suggest context-dependent roles of Runx2 via post-translational modifications during metastasis.

Runx2 functions at various stages of tumor progression as highlighted by several xenograft or genetic mouse models. The Runx2 overexpressing transgenic mice showed age-related pre-neoplastic changes in mammary epithelium.[15] Direct tibial inoculation of MDA-MB-231 cells with Runx2 knockdown (2 weeks) or miRNAs targeting Runx2 (4 weeks) showed reduced tumor growth and osteolysis.[28,66] The ectopic Runx2 expression in bone metastatic prostate cancer PC3 cells increased tumor growth when examined for 2 weeks.[65] Consistent with these studies, systemic inoculation of Runx2 knockdown cells showed delayed metastatic tumor growth at early time points (2 weeks) in our study. The reduction in tumor growth in the Runx2 knockdown group was compensated at later time points as these cells displayed regrowth in bone due to increased IGF-1Rβ. The results from these *in vivo* studies suggest that the route of cell injections, gene delivery method, tumor growth in visceral organs and bones, and the time required to reach the critical tumor size for osteolysis

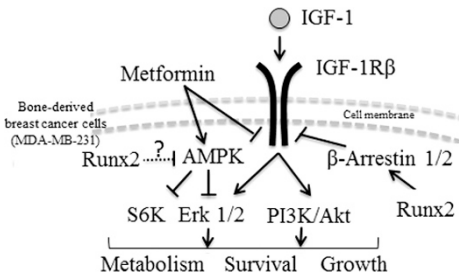

Figure 7. A schematic representation of Runx2 function in late-stage tumor growth in breast cancer bone metastasis. In bone-derived MDA-MB-231 cells, the IGF-mediated IGF-1Rβ phosphorylation triggers downstream PI3K/Akt activation to regulate cell growth. Runx2 inhibits IGF-1Rβ via β-Arrestin-1/2, but promotes pErk1/2 levels to regulate metabolism and cell survival. Runx2 also promotes glucose uptake and inhibits AMPK activation. Targeting Runx2-mediated IGF-1Rβ/Akt and AMPK/Erk crosstalk by metformin treatment reduces cell viability. The dotted lines represent possible indirect effect of Runx2.

may contribute to Runx2 response in tumor growth. Furthermore, these results highlight stage-specific adaptation of metastatic cancer cells in bone microenvironment via activation of IGF-1Rβ and AMPKβ signaling. The adaptation of cancer cells in metastatic microenvironment can be affected by the extent of AMPKα activation.[40] The increase in basal pAMPKα with Runx2 knockdown (Figures 6a–c) could allow bone-seeking cells to cope with stress and increase survival, as also seen in other cancer types during nutrient-deprivation conditions.[67,68] However, further increase in magnitude and duration of AMPKα activation by metformin could inhibit cell proliferation, cell cycle and survival.[42,43,69,70] Consistent with these results, we observed reduced viability of Runx2 knockdown cells with metformin treatment. Metformin indirectly promotes pAMPK by inhibiting complex I of the electron transport chain and increases AMP levels relative to ATP.[71,72] The increased pAMPKα levels in bone-derived Runx2 knockdown cells (Figures 6a–c) suggest altered AMP/ADP levels relative to ATP due to reduced glucose uptake (Figure 5b). The gene expression of LKB1, a serine/threonine kinase of AMPKα [73] and total AMPKα protein levels did not change significantly in Runx2 knockdown cells (data not shown and Supplementary Figure S5B) further support the indirect role of Runx2 on pAMPKα regulation. Importantly, our results demonstrating metformin-mediated potent reduction in IGF-1Rβ and Erk1/2 levels in bone-derived Runx2 knockdown cells indicate antitumor growth effects of metformin. Taken together, our results support targeting growth factor and metabolic signaling crosstalk using combinatorial approaches and repositioning of metformin for breast cancer bone metastasis.

MATERIALS AND METHODS

Cell lines, vectors and chemicals

The sources are listed in the supplementary section (Supplementary Table ST1). The MDA-MB-231, Hs578t and PC3 cells were cultured in minimum essential medium supplemented with 10% fetal bovine serum and 1% penicillin–streptomycin. For IGF-1 treatment, the cells were first serum deprived (0.25%) for 16 h. In experiments requiring, IGF-1Rβ inhibitor OSI-906/Linsitinib, PI3K inhibitor LY294002, Mek inhibitor UO126 or PD184161 treatment, the serum-deprived cells were pretreated with inhibitors for 10 min. The metformin was treated in serum- and glucose-deprived (100 mg/l) media.

The cell lines stably expressing Runx2 shRNA (Runx2-RNAi), WT-Runx2, firefly luciferase (Luc) and green fluorescent protein were generated utilizing lentivirus vectors.[14] The rat pcDNA3.1-β-Arrestin-1 expression plasmid was obtained from Addgene (Cambridge, MA, USA)[74] and transfected with lipofectamine LTX reagent, while pcDNA3 served as a vector control.

Bioluminescence imaging

All protocols were approved by RUSH University Medical Center Animal Care and Use committee. The six-week-old female NOD/SCID mice were obtained from Jackson Laboratories (Bar Harbor, ME, USA). MDA-MB-231 cells (10^5/100 μl) were inoculated intracardiacally into isoflurane anesthetized mice (10/group).[75,76] The mice were excluded from the study based on any sign of distress or infection. The tumor growth was weekly monitored by bioluminescence imaging (IVIS/Lumina; PerkinElmer, Waltham, MA, USA). The anesthetized mice were intraperitoneally inoculated with D-luciferin (3 mg/20 g) and the luminescent image was acquired. The region of interest was analyzed in a blinded manner using *Living Image* 4.1 software (PerkinElmer). To confirm the tumor location, mice were killed after 6 weeks, and organs were dissected and bioimaged. The experiments were repeated twice.

Radiography and μCT

The dorso-ventral radiographs were obtained using MX-20; Faxitron X-ray machine (Lincolnshire, IL, USA) at 20kV for 10 s. The designated bones (tibia and femur) were preserved in 10% formalin and stored in phosphate-buffered saline for μCT and histomorphometry. The μCT evaluation was performed in a blinded manner at Rush University's Histology Core Services.[77] The trabecular bone architecture parameters (bone volume fraction and trabecular connectivity) were obtained from the proximal tibia growth plate region.

Isolation of tumor cells

The tibia, femur and vertebrae were obtained from mice displaying osteolytic lesions. The cells were aseptically aspirated from bone marrow using a 28G needle. The vertebrae and lung were sliced, and incubated in collagenase and hyaloronidase containing growth media for 2 h. The cells were subsequently washed with phosphate-buffered saline, centrifuged and seeded. The fluorescence-activated cell sorting (green fluorescent protein) was performed at University of Illinois at Chicago. The single-cell colonies were isolated from 10^3 cells by performing serial 10-fold dilution. A 100 μl suspension of single cells was seeded on a 96-well plate and expanded.

Ex vivo tumor-bone co-culture

The tibia and femur were aseptically dissected and the proximal end was excised to reveal marrow cavity. The control or Runx2 knockdown MDA-MB-231 cells (2×10^4/10 μl) in serum-free media were inoculated into marrow using a $29^{1/2}$G needle. The bones with tumor cells were incubated for 2 weeks and bioimaged.

Western blotting and immunofluorescence

The western blot and immunofluorescence analysis were performed as previously described.[9,27] The antibodies are listed in Supplementary Table ST1.

Real-time PCR

The real-time PCR analysis was performed as previously described.[9] The primers (IDT, Coralville, IA, USA) are listed in Supplementary Table ST1. A human insulin pathway responsive PCR array was obtained from SA Biosciences (Qiagen, Valencia, CA, USA).

Luciferase assay

The TF search database was used to identify Runx-binding sites on β-Arrestin-1 promoter.[78] The WT or mutant β-Arrestin-1 promoters (+1–250 bp) were cloned in pcDNA3.1. The Runx2-binding consensus sequences, CA[79] were replaced by 'T' or 'G' in the mutant promoter (Supplementary Figure S4). The *firefly* and *renilla luciferase* plasmids were transfected using lipofectamine LTX and dual luciferase reporter assay (Promega, Madison, WI, USA) was performed.

Cell viability assay

The cell viability was determined by MTT assay (Promega) as previously described.[9]

In vitro clonogenic and soft agar assay

The clonogenic assays were performed by seeding 500 cells in a 100 mm dish for 12 days and colonies were stained with crystal violet (0.5 in 25% methanol). For soft agar assay, 5000 cells were plated in 0.35% agarose in growth media on top of solidified agarose (0.5%). The growth media was replaced every 3 days for 3 weeks.

Glucose uptake and glycolysis

The colorimetric glucose uptake assay was performed according to the manufacturer's guidelines (Sigma, St Louis, MO, USA). The glycolysis was determined as the extracellular acidification rate in response to glucose treatment in an XF-24 extracellular flux analyzer (Seahorse Bioscience, North Billerica, MA, USA). The MDA-MB-231 cells (4×10^4) were seeded in 96-well plates and serum-deprived overnight. The cells were rinsed with phosphate-buffered saline and incubated in glucose-free XF-assay medium. Subsequently, the cells were sequentially treated with glucose (10 mM), oligomycin (10 μM) and 2-DG (10 mM) in the analyzer and extracellular acidification rate values were recorded.

Statistical analysis

The data were analyzed by unpaired Student's *t*-test. $P \leq 0.05$ and $P \leq 0.1$ were considered as significant or marginally significant, respectively.

CONFLICT OF INTEREST

The authors declare no conflict of interest.

ACKNOWLEDGEMENTS

We thank Rush University Medical Center investigators; Dr Rick Sumner and his lab members, Dr Ryan Ross and Maleeha Mashiatulla for assistance with μCT data acquisition and analysis; Dr Amarjit Virdi for help with *the ex vivo* bone tumor co-culture model. We thank Dr Carl Maki and members of his lab, Dr Lei Duan and Ricardo Perez for helpful discussions throughout this study; Dr Elena Dedkova and Dr Lothar Blatter for assistance with sea horse data acquisition and analysis. This study was supported by the grant from Bears Care Foundation.

REFERENCES

1 Coleman RE, Rubens RD. The clinical course of bone metastases from breast cancer. *Br J Cancer* 1987; **55**: 61–66.
2 Ibrahim T, Mercatali L, Amadori D. A new emergency in oncology: bone metastases in breast cancer patients (Review). *Oncol Lett* 2013; **6**: 306–310.
3 Barnes GL, Hebert KE, Kamal M, Javed A, Einhorn TA, Lian JB *et al.* Fidelity of Runx2 activity in breast cancer cells is required for the generation of metastases-associated osteolytic disease. *Cancer Res* 2004; **64**: 4506–4513.
4 Mundy GR. Mechanisms of osteolytic bone destruction. *Bone* 1991; **12**(Suppl 1): S1–S6.
5 Chambers AF, Groom AC, MacDonald IC. Dissemination and growth of cancer cells in metastatic sites. *Nat Rev Cancer* 2002; **2**: 563–572.
6 Kingsley LA, Fournier PG, Chirgwin JM, Guise TA. Molecular biology of bone metastasis. *Mol Cancer Ther* 2007; **6**: 2609–2617.
7 Pande S, Browne G, Padmanabhan S, Zaidi SK, Lian JB, van Wijnen AJ *et al.* Oncogenic cooperation between PI3K/Akt signaling and transcription factor Runx2 promotes the invasive properties of metastatic breast cancer cells. *J Cell Physiol* 2013; **228**: 1784–1792.
8 Komori T, Yagi H, Nomura S, Yamaguchi A, Sasaki K, Deguchi K *et al.* Targeted disruption of Cbfa1 results in a complete lack of bone formation owing to maturational arrest of osteoblasts. *Cell* 1997; **89**: 755–764.
9 Tandon M, Chen Z, Pratap J. Runx2 activates PI3K/Akt signaling via mTORC2 regulation in invasive breast cancer cells. *Breast Cancer Res* 2014; **16**: R16.
10 Inman CK, Li N, Shore P. Oct-1 counteracts autoinhibition of Runx2 DNA binding to form a novel Runx2/Oct-1 complex on the promoter of the mammary gland-specific gene beta-casein. *Mol Cell Biol* 2005; **25**: 3182–3193.
11 Inman CK, Shore P. The osteoblast transcription factor Runx2 is expressed in mammary epithelial cells and mediates osteopontin expression. *J Biol Chem* 2003; **278**: 48684–48689.
12 Barnes GL, Javed A, Waller SM, Kamal MH, Hebert KE, Hassan MQ *et al.* Osteoblast-related transcription factors Runx2 (Cbfa1/AML3) and MSX2 mediate the expression of bone sialoprotein in human metastatic breast cancer cells. *Cancer Res* 2003; **63**: 2631–2637.
13 Martin TJ, Gillespie MT. Receptor activator of nuclear factor kappa B ligand (RANKL): another link between breast and bone. *Trends Endocrinol Metab* 2001; **12**: 2–4.
14 Pratap J, Imbalzano KM, Underwood JM, Cohet N, Gokul K, Akech J *et al.* Ectopic runx2 expression in mammary epithelial cells disrupts formation of normal acini structure: implications for breast cancer progression. *Cancer Res* 2009; **69**: 6807–6814.
15 McDonald L, Ferrari N, Terry A, Bell M, Mohammed ZM, Orange C *et al.* RUNX2 correlates with subtype-specific breast cancer in a human tissue microarray, and ectopic expression of Runx2 perturbs differentiation in the mouse mammary gland. *Dis Model Mech* 2014; **7**: 525–534.
16 Onodera Y, Miki Y, Suzuki T, Takagi K, Akahira J, Sakyu T *et al.* Runx2 in human breast carcinoma: its potential roles in cancer progression. *Cancer Sci* 2010; **101**: 2670–2675.
17 Pratap J, Galindo M, Zaidi SK, Vradii D, Bhat BM, Robinson JA *et al.* Cell growth regulatory role of Runx2 during proliferative expansion of preosteoblasts. *Cancer Res* 2003; **63**: 5357–5362.
18 Lucero CM, Vega OA, Osorio MM, Tapia JC, Antonelli M, Stein GS *et al.* The cancer-related transcription factor Runx2 modulates cell proliferation in human osteosarcoma cell lines. *J Cell Physiol* 2013; **228**: 714–723.
19 Chimge NO, Frenkel B. The RUNX family in breast cancer: relationships with estrogen signaling. *Oncogene* 2013; **32**: 2121–2130.
20 Roodman GD. Mechanisms of bone metastasis. *N Engl J Med* 2004; **350**: 1655–1664.
21 Hiraga T, Myoui A, Hashimoto N, Sasaki A, Hata K, Morita Y *et al.* Bone-derived IGF mediates crosstalk between bone and breast cancer cells in bony metastases. *Cancer Res* 2012; **72**: 4238–4249.
22 Riedemann J, Macaulay VM. IGF1R signalling and its inhibition. *Endocr Relat Cancer* 2006; **13**(Suppl 1): S33–S43.
23 Arteaga CL. Interference of the IGF system as a strategy to inhibit breast cancer growth. *Breast Cancer Res Treat* 1992; **22**: 101–106.
24 Dunn SE, Ehrlich M, Sharp NJ, Reiss K, Solomon G, Hawkins R *et al.* A dominant negative mutant of the insulin-like growth factor-I receptor inhibits the adhesion, invasion, and metastasis of breast cancer. *Cancer Res* 1998; **58**: 3353–3361.
25 Sachdev D, Zhang X, Matise I, Gaillard-Kelly M, Yee D. The type I insulin-like growth factor receptor regulates cancer metastasis independently of primary tumor growth by promoting invasion and survival. *Oncogene* 2010; **29**: 251–262.
26 Boroughs LK, DeBerardinis RJ. Metabolic pathways promoting cancer cell survival and growth. *Nat Cell Biol* 2015; **17**: 351–359.
27 Tandon M, Chen Z, Pratap J. Role of Runx2 in crosstalk between Mek/Erk and PI3K/Akt signaling in MCF-10A cells. *J Cell Biochem* 2014; **115**: 2208–2217.
28 Taipaleenmaki H, Browne G, Akech J, Zustin J, van Wijnen AJ, Stein JL *et al.* Targeting of Runx2 by miR-135 and miR-203 impairs progression of breast cancer and metastatic bone disease. *Cancer Res* 2015; **75**: 1433–1444.
29 Tandon M, Gokul K, Ali SA, Chen Z, Lian J, Stein GS *et al.* Runx2 mediates epigenetic silencing of the bone morphogenetic protein-3B (BMP-3B/GDF10) in lung cancer cells. *Mol Cancer* 2012; **11**: 27.
30 Leong DT, Lim J, Goh X, Pratap J, Pereira BP, Kwok HS *et al.* Cancer-related ectopic expression of the bone-related transcription factor RUNX2 in non-osseous metastatic tumor cells is linked to cell proliferation and motility. *Breast Cancer Res* 2010; **12**: R89.
31 Monami G, Emiliozzi V, Morrione A. Grb10/Nedd4-mediated multiubiquitination of the insulin-like growth factor receptor regulates receptor internalization. *J Cell Physiol* 2008; **216**: 426–437.
32 Aksamitiene E, Kiyatkin A, Kholodenko BN. Cross-talk between mitogenic Ras/MAPK and survival PI3K/Akt pathways: a fine balance. *Biochem Soc Trans* 2012; **40**: 139–146.
33 Oh JS, Kucab JE, Bushel PR, Martin K, Bennett L, Collins J *et al.* Insulin-like growth factor-1 inscribes a gene expression profile for angiogenic factors and cancer progression in breast epithelial cells. *Neoplasia* 2002; **4**: 204–217.
34 Kovacs JJ, Hara MR, Davenport CL, Kim J, Lefkowitz RJ. Arrestin development: emerging roles for beta-arrestins in developmental signaling pathways. *Dev Cell* 2009; **17**: 443–458.
35 Pratap J, Javed A, Languino LR, van Wijnen AJ, Stein JL, Stein GS *et al.* The Runx2 osteogenic transcription factor regulates matrix metalloproteinase 9 in bone metastatic cancer cells and controls cell invasion. *Mol Cell Biol* 2005; **25**: 8581–8591.
36 Berridge MV, Herst PM, Tan AS. Tetrazolium dyes as tools in cell biology: new insights into their cellular reduction. *Biotechnol Annu Rev* 2005; **11**: 127–152.
37 Robey IF, Lien AD, Welsh SJ, Baggett BK, Gillies RJ. Hypoxia-inducible factor-1alpha and the glycolytic phenotype in tumors. *Neoplasia* 2005; **7**: 324–330.
38 Robey IF, Stephen RM, Brown KS, Baggett BK, Gatenby RA, Gillies RJ. Regulation of the Warburg effect in early-passage breast cancer cells. *Neoplasia* 2008; **10**: 745–756.

39 Laderoute KR, Amin K, Calaoagan JM, Knapp M, Le T, Orduna J *et al.* 5'-AMP-activated protein kinase (AMPK) is induced by low-oxygen and glucose deprivation conditions found in solid-tumor microenvironments. *Mol Cell Biol* 2006; **26**: 5336–5347.
40 Liang J, Mills GB. AMPK: a contextual oncogene or tumor suppressor? *Cancer Res* 2013; **73**: 2929–2935.
41 Liu B, Fan Z, Edgerton SM, Deng XS, Alimova IN, Lind SE *et al.* Metformin induces unique biological and molecular responses in triple negative breast cancer cells. *Cell Cycle* 2009; **8**: 2031–2040.
42 Zhuang Y, Miskimins WK. Cell cycle arrest in Metformin treated breast cancer cells involves activation of AMPK, downregulation of cyclin D1, and requires p27Kip1 or p21Cip1. *J Mol Signal* 2008; **3**: 18.
43 Zordoky BN, Bark D, Soltys CL, Sung MM, Dyck JR. The anti-proliferative effect of metformin in triple-negative MDA-MB-231 breast cancer cells is highly dependent on glucose concentration: implications for cancer therapy and prevention. *Biochim Biophys Acta* 2014; **1840**: 1943–1957.
44 Liu X, Chhipa RR, Nakano I, Dasgupta B. The AMPK inhibitor compound C is a potent AMPK-independent antiglioma agent. *Mol Cancer Ther* 2014; **13**: 596–605.
45 Henkels KM, Mallets ER, Dennis PB, Gomez-Cambronero J. S6K is a morphogenic protein with a mechanism involving Filamin-A phosphorylation and phosphatidic acid binding. *FASEB J* 2015; **29**: 1299–1313.
46 Foley J, Nickerson NK, Nam S, Allen KT, Gilmore JL, Nephew KP *et al.* EGFR signaling in breast cancer: bad to the bone. *Semin Cell Dev Biol* 2010; **21**: 951–960.
47 Suva LJ, Washam C, Nicholas RW, Griffin RJ. Bone metastasis: mechanisms and therapeutic opportunities. *Nat Rev Endocrinol* 2011; **7**: 208–218.
48 Guise T. Examining the metastatic niche: targeting the microenvironment. *Semin Oncol* 2010; **37**(Suppl 2): S2–S14.
49 Xian L, Wu X, Pang L, Lou M, Rosen CJ, Qiu T *et al.* Matrix IGF-1 maintains bone mass by activation of mTOR in mesenchymal stem cells. *Nat Med* 2012; **18**: 1095–1101.
50 Taniguchi CM, Emanuelli B, Kahn CR. Critical nodes in signalling pathways: insights into insulin action. *Nat Rev Mol Cell Biol* 2006; **7**: 85–96.
51 Yee D. Insulin-like growth factor receptor inhibitors: baby or the bathwater? *J Natl Cancer Inst* 2012; **104**: 975–981.
52 Thirunavukkarasu K, Mahajan M, McLarren KW, Stifani S, Karsenty G. Two domains unique to osteoblast-specific transcription factor Osf2/Cbfa1 contribute to its transactivation function and its inability to heterodimerize with Cbfbeta. *Mol Cell Biol* 1998; **18**: 4197–4208.
53 Westendorf JJ. Transcriptional co-repressors of Runx2. *J Cell Biochem* 2006; **98**: 54–64.
54 Franceschi RT, Ge C, Xiao G, Roca H, Jiang D. Transcriptional regulation of osteoblasts. *Cells Tissues Organs* 2009; **189**: 144–152.
55 Jonason JH, Xiao G, Zhang M, Xing L, Chen D. Post-translational regulation of Runx2 in bone and cartilage. *J Dent Res* 2009; **88**: 693–703.
56 Oakley RH, Revollo J, Cidlowski JA. Glucocorticoids regulate arrestin gene expression and redirect the signaling profile of G protein-coupled receptors. *Proc Natl Acad Sci USA* 2012; **109**: 17591–17596.
57 Westendorf JJ, Zaidi SK, Cascino JE, Kahler R, van Wijnen AJ, Lian JB *et al.* Runx2 (Cbfa1, AML-3) interacts with histone deacetylase 6 and represses the p21 (CIP1/WAF1) promoter. *Mol Cell Biol* 2002; **22**: 7982–7992.
58 Lian JB, Stein JL, Stein GS, van Wijnen AJ, Montecino M, Javed A *et al.* Runx2/Cbfa1 functions: diverse regulation of gene transcription by chromatin remodeling and co-regulatory protein interactions. *Connect Tissue Res* 2003; **44** (Suppl 1): 141–148.
59 Boumah CE, Lee M, Selvamurugan N, Shimizu E, Partridge NC. Runx2 recruits p300 to mediate parathyroid hormone's effects on histone acetylation and transcriptional activation of the matrix metalloproteinase-13 gene. *Mol Endocrinol* 2009; **23**: 1255–1263.
60 Ali SA, Dobson JR, Lian JB, Stein JL, van Wijnen AJ, Zaidi SK *et al.* A RUNX2-HDAC1 co-repressor complex regulates rRNA gene expression by modulating UBF acetylation. *J Cell Sci* 2012; **125**(Pt 11): 2732–2739.
61 Ozaki T, Wu D, Sugimoto H, Nagase H, Nakagawara A. Runt-related transcription factor 2 (RUNX2) inhibits p53-dependent apoptosis through the collaboration with HDAC6 in response to DNA damage. *Cell Death Dis* 2013; **4**: e610.
62 Wu H, Whitfield TW, Gordon JA, Dobson JR, Tai PW, van Wijnen AJ *et al.* Genomic occupancy of Runx2 with global expression profiling identifies a novel dimension to control of osteoblastogenesis. *Genome Biol* 2014; **15**: R52.
63 Ge C, Xiao G, Jiang D, Franceschi RT. Critical role of the extracellular signal-regulated kinase-MAPK pathway in osteoblast differentiation and skeletal development. *J Cell Biol* 2007; **176**: 709–718.
64 Ge C, Xiao G, Jiang D, Yang Q, Hatch NE, Roca H *et al.* Identification and functional characterization of ERK/MAPK phosphorylation sites in the Runx2 transcription factor. *J Biol Chem* 2009; **284**: 32533–32543.
65 Ge C, Zhao G, Li Y, Li H, Zhao X, Pannone G *et al.* Role of Runx2 phosphorylation in prostate cancer and association with metastatic disease. *Oncogene* 2016; **35**: 366–376.
66 Pratap J, Wixted JJ, Gaur T, Zaidi SK, Dobson J, Gokul KD *et al.* Runx2 transcriptional activation of Indian Hedgehog and a downstream bone metastatic pathway in breast cancer cells. *Cancer Res* 2008; **68**: 7795–7802.
67 Kato K, Ogura T, Kishimoto A, Minegishi Y, Nakajima N, Miyazaki M *et al.* Critical roles of AMP-activated protein kinase in constitutive tolerance of cancer cells to nutrient deprivation and tumor formation. *Oncogene* 2002; **21**: 6082–6090.
68 Park HU, Suy S, Danner M, Dailey V, Zhang Y, Li H *et al.* AMP-activated protein kinase promotes human prostate cancer cell growth and survival. *Mol Cancer Ther* 2009; **8**: 733–741.
69 Zhuang Y, Miskimins WK. Metformin induces both caspase-dependent and poly (ADP-ribose) polymerase-dependent cell death in breast cancer cells. *Mol Cancer Res* 2011; **9**: 603–615.
70 Morales DR, Morris AD. Metformin in cancer treatment and prevention. *Annu Rev Med* 2015; **66**: 17–29.
71 Dowling RJ, Goodwin PJ, Stambolic V. Understanding the benefit of metformin use in cancer treatment. *BMC Med* 2011; **9**: 33.
72 Hatoum D, McGowan EM. Recent advances in the use of metformin: can treating diabetes prevent breast cancer? *Biomed Res Int* 2015; **2015**: 548436.
73 Taliaferro-Smith L, Nagalingam A, Zhong D, Zhou W, Saxena NK, Sharma D. LKB1 is required for adiponectin-mediated modulation of AMPK-S6K axis and inhibition of migration and invasion of breast cancer cells. *Oncogene* 2009; **28**: 2621–2633.
74 Hara MR, Kovacs JJ, Whalen EJ, Rajagopal S, Strachan RT, Grant W *et al.* A stress response pathway regulates DNA damage through beta2-adrenoreceptors and beta-arrestin-1. *Nature* 2011; **477**: 349–353.
75 Kang Y, Siegel PM, Shu W, Drobnjak M, Kakonen SM, Cordon-Cardo C *et al.* A multigenic program mediating breast cancer metastasis to bone. *Cancer Cell* 2003; **3**: 537–549.
76 Campbell JP, Merkel AR, Masood-Campbell SK, Elefteriou F, Sterling JA. Models of bone metastasis. *J Vis Exp* 2012; e-pub ahead of print 4 September 2014; doi: 10.3791/4260.
77 Ross RD, Edwards LH, Acerbo AS, Ominsky MS, Virdi AS, Sena K *et al.* Bone matrix quality after sclerostin antibody treatment. *J Bone Miner Res* 2014; **29**: 1597–1607.
78 Wingender E, Kel AE, Kel OV, Karas H, Heinemeyer T, Dietze P *et al.* TRANSFAC, TRRD and COMPEL: towards a federated database system on transcriptional regulation. *Nucleic Acids Res* 1997; **25**: 265–268.
79 Drissi H, Pouliot A, Stein JL, van Wijnen AJ, Stein GS, Lian JB. Identification of novel protein/DNA interactions within the promoter of the bone-related transcription factor Runx2/Cbfa1. *J Cell Biochem* 2002; **86**: 403–412.

Supplementary Information accompanies this paper on the Oncogene website (http://www.nature.com/onc)